IOP PUBLISHING EUROPEAN JOURNAL OF PHYSICS

Eur. J. Phys. **30** (2009) 661–675 doi:10.1088/0143-0807/30/4/001

The elusive memristor: properties of basic electrical circuits

Yogesh N Joglekar and Stephen J Wolf

Department of Physics, Indiana University Purdue University Indianapolis, Indianapolis, IN 46202, USA

E-mail: yojoglek@iupui.edu

Received 13 January 2009, in final form 25 March 2009
Published 5 May 2009
Online at stacks.iop.org/EJP/30/661

Abstract

We present an introduction to and a tutorial on the properties of the recently discovered ideal circuit element, a memristor. By definition, a memristor M relates the charge q and the magnetic flux ϕ in a circuit and complements a resistor R, a capacitor C and an inductor L as an ingredient of ideal electrical circuits. The properties of these three elements and their circuits are a part of the standard curricula. The existence of the memristor as the fourth ideal circuit element was predicted in 1971 based on symmetry arguments, but was clearly experimentally demonstrated just last year. We present the properties of a single memristor, memristors in series and parallel, as well as ideal memristor–capacitor (MC), memristor–inductor (ML) and memristor–capacitor–inductor (MCL) circuits. We find that the memristor has hysteretic current–voltage characteristics. We show that the ideal MC (ML) circuit undergoes non-exponential charge (current) decay with two time scales and that by switching the polarity of the capacitor, an ideal MCL circuit can be tuned from overdamped to underdamped. We present simple models which show that these unusual properties are closely related to the memristor's internal dynamics. This tutorial complements the pedagogy of ideal circuit elements (R, C and L) and the properties of their circuits, and is aimed at undergraduate physics and electrical engineering students.

(Some figures in this article are in colour only in the electronic version)

1. Introduction

The properties of basic electrical circuits, constructed from three ideal elements, a resistor, a capacitor, an inductor and an ideal voltage source $v(t)$ are a standard staple of physics and engineering courses. These circuits show a wide variety of phenomena such as the exponential charging and discharging of a resistor–capacitor (RC) circuit with time constant $\tau_{RC} = RC$, the exponential rise and decay of the current in a resistor–inductor (RL) circuit with time

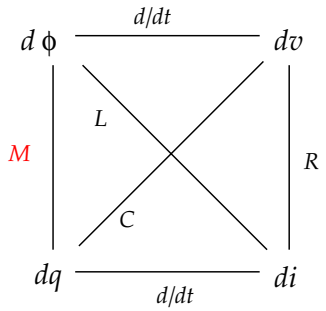

Figure 1. Relations between four variables of basic electrical circuit theory: the charge q, current i, voltage v and the magnetic flux ϕ. Three well-known ideal circuit elements R, C and L are associated with pairs $(\mathrm{d}v, \mathrm{d}i)$, $(\mathrm{d}q, \mathrm{d}v)$ and $(\mathrm{d}\phi, \mathrm{d}i)$, respectively. The top (bottom) horizontal pair is related by Lenz's law (definition). This leaves the pair $(\mathrm{d}\phi, \mathrm{d}q)$ unrelated. Leon Chua postulated that, due to symmetry, the fourth ideal element (memristor) that relates this pair, $\mathrm{d}\phi = M\,\mathrm{d}q$, must exist.

constant $\tau_{RL} = L/R$, the non-dissipative oscillations in an inductor–capacitor (LC) circuit with frequency $\omega_{LC} = 1/\sqrt{LC}$ as well as resonant oscillations in a resistor–capacitor–inductor (RCL) circuit induced by an alternating-current (ac) voltage source with frequency $\omega \sim \omega_{LC}$ [1]. The behaviour of these ideal circuits is determined by Kirchoff's current law that follows from the continuity equation and Kirchoff's voltage law. We remind the reader that Kirchoff's voltage law follows from Maxwell's second equation only when the time dependence of the magnetic field created by the current in the circuit is ignored, $\oint \mathbf{E}\cdot\mathbf{dl} = 0$ where the line integral of the electric field $\mathbf{E}$ is taken over any closed loop in the circuit [2]. The study of elementary circuits with ideal elements provides us with a recipe to understand real-world circuits where every capacitor has a finite resistance, every battery has an internal resistance and every resistor has an inductive component; we assume that the real-world circuits can be modelled using only the three ideal elements and an ideal voltage source.

An ideal capacitor is defined by the single-valued relationship between the charge $q(t)$ and the voltage $v(t)$ via $\mathrm{d}v = \mathrm{d}q/C(q)$. Similarly, an ideal resistor is defined by a single-valued relationship between the current $i(t)$ and the voltage $v(t)$ via $\mathrm{d}v = R(i)\,\mathrm{d}i$, and an ideal inductor is defined by a single-valued relationship between the magnetic flux $\phi(t)$ and the current $i(t)$ via $\mathrm{d}\phi = L(i)\,\mathrm{d}i$. These three definitions provide three relations between the four fundamental constituents of the circuit theory, namely the charge q, current i, voltage v and magnetic flux ϕ (see figure 1). The definition of current, $i = \mathrm{d}q/\mathrm{d}t$, and the Lenz's law, $v = +\mathrm{d}\phi/\mathrm{d}t$, give two more relations between the four constituents. (We define the flux such that the sign in the Lenz law is positive.) These five relations, shown in figure 1, raise a natural question: Is there an ideal element that relates the charge $q(t)$ and magnetic flux $\phi(t)$? Based on this symmetry argument, in 1971 Chua postulated that a new ideal element defined by the single-valued relationship $\mathrm{d}\phi = M(q)\,\mathrm{d}q$ must exist. He called this element memristor, M, short for memory resistor [3]. This ground-breaking hypothesis meant that the trio of ideal circuit elements (R, C, L) were not sufficient to model a basic real-world circuit (that may have a memristive component as well). In 1976, Chua and Kang extended the analysis further to memristive systems [4, 5]. These seminal papers studied the properties of a memristor, the fourth ideal circuit element, and showed that diverse systems such as thermistors, Josephson junctions and ionic transport in neurons, described by the Hodgkins–Huxley model, are special cases of memristive systems [3–5].

Despite the simplicity and the soundness of the symmetry argument that predicts the existence of the fourth ideal element, experimental realization of a quasi-ideal memristor—defined by the single-valued relationship $\mathrm{d}\phi = M(q)\,\mathrm{d}q$—remained elusive[1]. In 2008, Strukov and co-workers [9] created, using a nanoscale thin-film device, the first realization of a memristor. They presented an elegant physical model in which the memristor is equivalent to a time-dependent resistor whose value at time t is linearly proportional to the amount of charge $q(t)$ that has passed through it before. This equivalence follows from the memristor's definition and Lenz's law, $\mathrm{d}\phi = M(q)\,\mathrm{d}q \Leftrightarrow v = M(q)i$. It also implies that the memristor value—memristance—is measured in the same units as the resistance.

In this paper, we present the properties of basic electrical circuits with a memristor. For the most part, this theoretical investigation uses Kirchoff's law and Ohm's law. In the following section, we discuss the memristor model presented in [9] and analytically derive its i–v characteristics. Section 3 contains theoretical results for ideal MC and ML circuits. We use the linear-drift model, presented in [9], to describe the dependence of the effective resistance of the memristor (memristance) on the charge that has passed through it. This simplification allows us to obtain analytical closed-form results. We show that the charge (current) decay 'time-constant' in an ideal MC (ML) circuit depends on the polarity of the memristor. Section 4 is intended for advanced students. In this section, we present models that characterize the dependence of the memristance on the dopant drift inside the memristor. We show that the memristive behaviour is amplified when we use models that are more realistic than that used in preceding sections. In section 5 we discuss an ideal MCL circuit. We show that depending on the polarity of the memristor, the MCL circuit can be overdamped or underdamped, and thus allows far more tunability than an ideal RCL circuit. Section 6 concludes the tutorial with a brief discussion. This tutorial adds to the pedagogy of undergraduate physics and electrical engineering.

2. A single memristor

We start this section with the elegant model of a memristor presented in [9]. It consisted of a thin film (5 nm thick) with one layer of insulating TiO_2 and oxygen-poor TiO_{2-x} each, sandwiched between platinum contacts [10]. The oxygen vacancies in the second layer behave as charge +2 mobile dopants. These dopants create a doped TiO_2 region, whose resistance is significantly lower than the resistance of the undoped region. The boundary between the doped and undoped regions, and therefore the effective resistance of the thin film, depends on the position of these dopants. It, in turn, is determined by their mobility[2] μ_D ($\sim 10^{-10}$ cm^2 V^{-1} s^{-1}) [9] and the electric field across the doped region. Since it is not trivial to obtain the microscopic dopant density profile, we characterize the time evolution of this profile by the average dopant velocity. Figure 2 shows a schematic of a memristor of size D ($D \sim 10$ nm) modelled as two resistors in series, the doped region with size w and the undoped region with size $(D - w)$. The effective resistance of such a device is

$$M(w) = \frac{w}{D}\mathcal{R}_{\mathrm{ON}} + \left(1 - \frac{w}{D}\right)\mathcal{R}_{\mathrm{OFF}}, \tag{1}$$

where $\mathcal{R}_{\mathrm{ON}}$ (~ 1 kΩ) [9] is the resistance of the memristor if it is completely doped and $\mathcal{R}_{\mathrm{OFF}}$ is its resistance if it is undoped. Although equation (1) is valid for arbitrary values of $\mathcal{R}_{\mathrm{ON}}$

[1] Over the last two decades, devices with programmable variable resistance, also called memristors, have been fabricated [6–8]. They show hysteretic i–v characteristics, but do not discuss the defining property of a memristor, the invertible relationship between the charge and the magnetic flux. The interplay between electronic and ionic transport in these samples is non-trivial, and none of them have presented a simple physical picture similar to that in [9].

[2] For an introduction to semiconductors and mobility, see chapters 42 and 25 of the second part of [1].

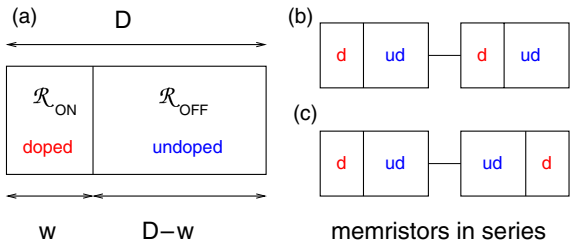

Figure 2. (a) Schematic of a memristor of length D as two resistors in series. The doped region (TiO_{2-x}) has resistance $\mathcal{R}_{ON}w/D$ and the undoped region (TiO_2) has resistance $\mathcal{R}_{OFF}(1-w/D)$. The size of the doped region, with its charge +2 ionic dopants, changes in response to the applied voltage and thus alters the effective resistance of the memristor. (b) Two memristors with the same polarity in series. d and ud represent the doped and undoped regions, respectively. In this case, the memristive effect is retained because doped regions in both memristors simultaneously shrink or expand. (c) Two memristors with opposite polarities in series. The net memristive effect is suppressed.

and $\mathcal{R}_{OFF}$, experimentally, the resistance of the doped TiO_2 film is significantly smaller than the undoped film, $\mathcal{R}_{OFF}/\mathcal{R}_{ON} \sim 10^2 \gg 1$ and therefore $\Delta\mathcal{R} = (\mathcal{R}_{OFF} - \mathcal{R}_{ON}) \approx \mathcal{R}_{OFF}$. In the presence of a voltage $v(t)$, the current in the memristor is determined by Kirchoff's voltage law $v(t) = M(w)i(t)$. The memristive behaviour of this system is reflected in the time dependence of size of the doped region $w(t)$. In the simplest model—the linear-drift model—the boundary between the doped and undoped regions drifts at a constant speed v_D given by

$$\frac{dw}{dt} = v_D = \eta\frac{\mu_D\mathcal{R}_{ON}}{D}i(t), \tag{2}$$

where we have used the fact that a current $i(t)$ corresponds to a uniform electric field $\mathcal{R}_{ON}i(t)/D$ across the doped region. Since the (oxygen vacancy) dopant drift can either expand or contract the doped region, we characterize the 'polarity' of a memristor by $\eta = \pm 1$, where $\eta = +1$ corresponds to the expansion of the doped region. We note that 'switching the memristor polarity' means reversing the battery terminals, or the $\pm$ plates of a capacitor (in an MC circuit) or reversing the direction of the initial current (in an ML circuit). Equations (1) and (2) are used to determine the i–v characteristics of a memristor. Integrating equation (2) gives

$$w(t) = w_0 + \eta\frac{\mu_D\mathcal{R}_{ON}}{D}q(t) = w_0 + \eta\frac{Dq(t)}{Q_0}, \tag{3}$$

where w_0 is the initial size of the doped region. Thus, the width of the doped region $w(t)$ changes linearly[3] with the amount of charge that has passed through it. $Q_0 = D^2/\mu_D\mathcal{R}_{ON}$ is the charge that is required to pass through the memristor for the dopant boundary to move through distance D (typical parameters [9] imply $Q_0 \sim 10^{-2}$ C). It provides the natural scale for charge in a memristive circuit. Substituting this result into equation (1) gives

$$M(q) = \mathcal{R}_0 - \eta\frac{\Delta\mathcal{R}q}{Q_0}, \tag{4}$$

[3] The linear-drift model is valid only when $0 \leqslant w(t) \leqslant D$ for all t. This constraint provides limits on the flux ϕ, the initial capacitor charge q_0 or the dc voltage v_0 and the initial current i_0. We compare linear and nonlinear dopant drift models in section 4.

where $\mathcal{R}_0 = \mathcal{R}_{\rm ON}(w_0/D) + \mathcal{R}_{\rm OFF}(1 - w_0/D)$ is the effective resistance (memristance) at time $t = 0$. Equation (4) shows explicitly that the memristance $M(q)$ depends purely on the charge q that has passed through it. Combined with $v(t) = M(q)i(t)$, equation (4) implies that the model presented here is an ideal memristor. (We recall that $v = M(q)i$ is equivalent to $\mathrm{d}\phi = M\,\mathrm{d}q$.) The prefactor of the q-dependent term is proportional to $1/D^2$ and becomes increasingly important when D is small. In addition, for a given D, the memristive effects become important only when $\Delta\mathcal{R} \gg \mathcal{R}_0$. Now that we have discussed the memristor model from [9], in the following paragraphs we obtain analytical results for its i–v characteristics.

For an ideal circuit with a single memristor and a voltage supply, Kirchoff's voltage law implies

$$\left(\mathcal{R}_0 - \eta\frac{\Delta\mathcal{R}q(t)}{Q_0}\right)\frac{\mathrm{d}q}{\mathrm{d}t} = \frac{\mathrm{d}}{\mathrm{d}t}\left(\mathcal{R}_0 q - \eta\frac{\Delta\mathcal{R}q^2}{2Q_0}\right) = v(t). \tag{5}$$

The solution of this equation, subject to the boundary condition $q(0) = 0$, is

$$q(t) = \frac{Q_0\mathcal{R}_0}{\Delta\mathcal{R}}\left[1 - \sqrt{1 - \eta\frac{2\Delta\mathcal{R}}{Q_0\mathcal{R}_0^2}\phi(t)}\right], \tag{6}$$

$$i(t) = \frac{v(t)}{\mathcal{R}_0}\frac{1}{\sqrt{1 - 2\eta\Delta\mathcal{R}\phi(t)/Q_0\mathcal{R}_0^2}} = \frac{v(t)}{M(q(t))}, \tag{7}$$

where $\phi(t) = \int_0^t \mathrm{d}\tau\, v(\tau)$ is the magnetic flux associated with the voltage $v(t)$. Equations (6) and (7) provide analytical results for i–v characteristics of an ideal memristor circuit. Equation (6) shows that the charge is an invertible function of the magnetic flux [3, 4] consistent with the defining equation $\mathrm{d}\phi = M(q)\,\mathrm{d}q$. Equation (7) shows that $i = 0$ if and only if $v = 0$. Therefore, unlike an ideal capacitor or an inductor, the memristor is a purely dissipative element [3]. For an ac voltage $v(t) = v_0\sin(\omega t)$, the magnetic flux is $\phi(t) = v_0[1 - \cos(\omega t)]/\omega$. Although $v(\pi/\omega - t) = v(t)$, $\phi(\pi/\omega - t) \neq \phi(t)$; therefore, it follows from equation (7) that the current $i(v)$ will be a multi-valued function of the voltage v. Note that even though the voltage has a single Fourier frequency component at ω, the current $i(t)$ has multiple Fourier components. It also follows that since $\phi \propto 1/\omega$, the memristive behaviour is dominant only at low frequencies $\omega \lesssim \omega_0 = 2\pi/t_0$. Here $t_0 = D^2/\mu_D v_0$ is the time that the dopants need to travel distance D under a constant voltage v_0. t_0 and ω_0 provide the natural time and frequency scales for a memristive circuit (typical parameters [9] imply $t_0 \sim 0.1$ ms and $\omega_0 \sim 50$ KHz). We emphasize that equation (6) is based on the linear-drift model, equation (2), and is valid only when the charge flowing through the memristor is less than $q_{\max}(t) = Q_0(1 - w_0/D)$ when $\eta = +1$ or $q_{\max}(t) = Q_0 w_0/D$ when $\eta = -1$. It is easy to obtain a diversity of i–v characteristics using equations (6) and (7), including those presented in [9, 10] by choosing appropriate functional forms of $v(t)$. Figure 3 shows the theoretical i–v curves for $v(t) = v_0\sin(\omega t)$ for $\omega = 0.5\omega_0$ (red solid), $\omega = \omega_0$ (green dashed) and $\omega = 5\omega_0$ (blue dotted). In each case, the high initial resistance $\mathcal{R}_0$ leads to the small slope of the i–v curves at the beginning. For $\omega \leqslant \omega_0$ as the voltage increases, the size of the doped region increases and the memristance decreases. Therefore, the slope of the i–v curve on the return sweep is large, creating a hysteresis loop. The size of this loop varies inversely with the frequency ω. At high frequencies, $\omega = 5\omega_0$, the size of the doped region barely changes before the applied voltage begins the return sweep. Hence the memristance remains essentially unchanged and the hysteretic behaviour is suppressed. The inset in figure 3 shows the theoretical q–ϕ curve for $\omega = 0.5\omega_0$ that follows from equation (6).

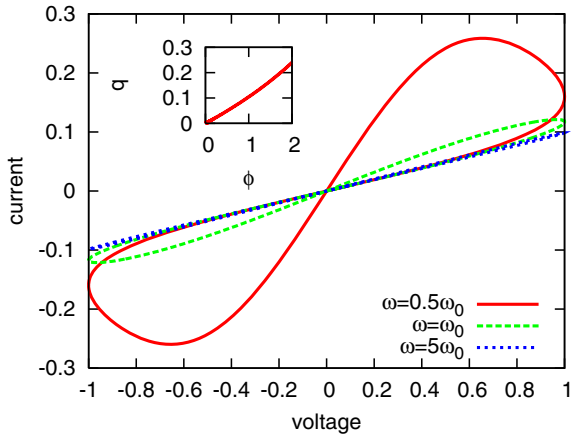

Figure 3. Theoretical i–v characteristics of a memristor with applied voltage $v(t) = v_0 \sin(\omega t)$ for $\omega = 0.5\omega_0$ (red solid), $\omega = \omega_0$ (green dashed) and $\omega = 5\omega_0$ (blue dotted). The memristor parameters are $w_0/D = 0.5$ and $\mathcal{R}_{\rm OFF}/\mathcal{R}_{\rm ON} = 20$. The unit of resistance is $\mathcal{R}_{\rm ON}$, the unit of voltage is v_0 and the unit of current is $I_0 = Q_0/t_0$. We see that the hysteresis is pronounced for $\omega \leqslant \omega_0$ and suppressed when $\omega \gg \omega_0$. The inset is a typical q–ϕ graph showing that the charge q is an invertible function of the flux ϕ. The unit of flux $\phi_0 = v_0 t_0 = D^2/\mu_D$ is determined by the memristor properties alone (typical parameters [9] imply $\phi_0 = 10^{-2}$ Wb).

Thus, a single memristor shows a wide variety of i–v characteristics based on the frequency of the applied voltage. Since the mobility of the (oxygen vacancy) dopants is low, memristive effects are appreciable only when the memristor size is nanoscale. Now, we consider an ideal circuit with two memristors in series (figure 2). It follows from Kirchoff's laws that if two memristors M_1 and M_2 have the same polarity, $\eta_1 = \eta_2$, they add like regular resistors, $M(q) = (\mathcal{R}_{01} + \mathcal{R}_{02}) - \eta(\Delta\mathcal{R}_1 + \Delta\mathcal{R}_2)q(t)/Q_0$ whereas when they have opposite polarities, $\eta_1\eta_2 = -1$, the q-dependent component is suppressed, $M(q) = (\mathcal{R}_{01} + \mathcal{R}_{02}) - \eta(\Delta\mathcal{R}_1 - \Delta\mathcal{R}_2)q(t)/Q_0$. The fact that memristors with the same polarities add in series leads to the possibility of a superlattice of memristors with micron dimensions instead of nanoscale dimensions. We emphasize that a single memristor cannot be scaled up without losing the memristive effect because the relative change in the size of the doped region decreases with scaling. A superlattice of nanoscale memristors, on the other hand, will show the same memristive effect when scaled up. We leave the problem of two memristors in parallel to the reader.

These non-trivial properties of an ideal memristor circuit raise the following question: What are the properties of basic circuits with a memristor and a capacitor or an inductor? (A memristor–resistor circuit is trivial.) We will explore this question in the subsequent sections.

3. Ideal MC and ML circuits

Let us consider an ideal MC circuit with a capacitor having an initial charge q_0 and no voltage source. The effective resistance of the memristor is determined by its polarity (whether the doped region increases or decreases), and since the charge decay time-constant of the MC circuit depends on its effective resistance, the capacitor discharge will depend on the memristor polarity. Kirchoff's voltage law applied to an ideal MC circuit gives

$$M_c(q(t))\frac{{\rm d}q}{{\rm d}t} + \frac{q}{C} = 0, \tag{8}$$

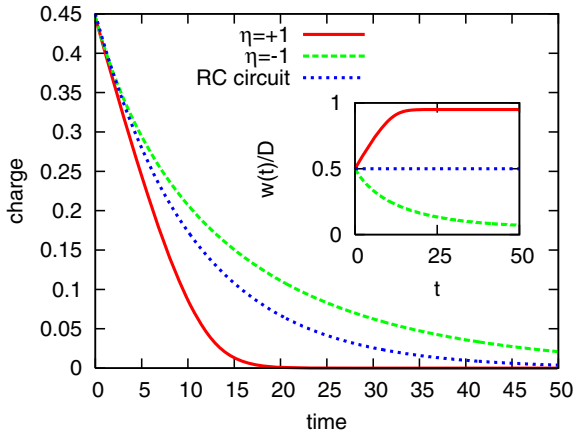

Figure 4. Theoretical q–t characteristics of an ideal MC circuit. The memristor parameters are $w_0/D = 0.5$ and $\mathcal{R}_{\rm OFF}/\mathcal{R}_{\rm ON} = 20$. The initial charge on the capacitor is $q_0/Q_0 = 0.45 < (1 - w_0/D)$ to ensure the validity of the linear-drift model and $C/C_0 = 1$. The unit of capacitance is $C_0 = Q_0/v_0 = t_0/\mathcal{R}_{\rm ON}$. We see that when $\eta = +1$ (red solid), the capacitor charge in the MC circuit decays about *twice as fast* as when $\eta = -1$ (green dashed). The central blue dotted plot shows the exponential charge decay of an RC circuit with the same initial resistance $\mathcal{R}_0$. The inset shows the time evolution of the boundary between the doped and undoped regions when $\eta = +1$ (red solid) and $\eta = -1$ (green dashed), and confirms that the linear-drift model is valid.

where $q(t)$ is the charge on the capacitor. We emphasize that the q-dependence of the memristance here is $M_c(q) = \mathcal{R}_0 - \eta\Delta\mathcal{R}(q_0 - q)/Q_0$ because if q is the remaining charge on the capacitor, then the charge that has passed through the memristor is $(q_0 - q)$. Equation (8) is integrated by rewriting it as $\mathrm{d}q/\mathrm{d}t = -q/(a + bq)$, where $a = C(\mathcal{R}_0 - \eta\Delta\mathcal{R}q_0/Q_0)$ and $b = \eta C\Delta\mathcal{R}/Q_0$. We obtain the following implicit equation:

$$q(t)\exp\left[\frac{\eta\Delta\mathcal{R}q(t)}{\mathcal{R}_F Q_0}\right] = q_0\exp\left[-\frac{t}{\mathcal{R}_F C}\right]\exp\left[\frac{\eta\Delta\mathcal{R}q_0}{\mathcal{R}_F Q_0}\right], \tag{9}$$

where $\mathcal{R}_F = \mathcal{R}_0 - \eta\Delta\mathcal{R}q_0/Q_0$ is the memristance when the entire charge q_0 has passed through the memristor. A small t-expansion of equation (9) shows that the initial current $i(0) = q_0/\mathcal{R}_0 C$ is independent of the memristor polarity η, and the large-t expansion shows that the charge on the capacitor decays exponentially, $q(t \to \infty) = q_0\exp(-t/\mathcal{R}_F C)\exp(\eta\Delta\mathcal{R}q_0/\mathcal{R}_F Q_0)$. In the intermediate region, the naive expectation $q(t) = q_0\exp[-t/M(w(t))C]$ is not the self-consistent solution of equation (9). Therefore, although a memristor can be thought of as an effective resistor, its effect in an MC circuit is not captured by merely substituting its time-dependent value in place of the resistance in an ideal RC circuit. Qualitatively, since the memristance decreases or increases depending on its polarity, we expect that when $\eta = +1$ the MC circuit will discharge faster than an RC circuit with the same resistance $\mathcal{R}_0$. This RC circuit, in turn, will discharge faster than the same MC circuit when $\eta = -1$. Figure 4 shows the theoretical q–t curves obtained by (numerically) integrating equation (8). These results indeed fulfil our expectations. We note that equation (9), obtained using the linear-drift model, is valid for $q_0 \leqslant Q_0(1 - w_0/D)$ when $\eta = +1$ which guarantees that the final memristance $\mathcal{R}_F \geqslant \mathcal{R}_{\rm ON}$ is always positive. The inset shows the time evolution of the size of the doped region $w(t)$ obtained using equation (3) and confirms the applicability of the linear-drift model. We remind the reader that changing the polarity of the memristor can be accomplished by exchanging the $\pm$ plates of the fully charged capacitor.

It is now straightforward to understand an ideal MC circuit with a direct current (dc) voltage source v_0 and an uncharged capacitor. This problem is the time-reversed version of an MC circuit with the capacitor charge $q_0 = v_0 C$ and no voltage source. The only salient difference is that in the present case, the charge passing through the memristor is the same as the charge on the capacitor. Using Kirchoff's voltage law we obtain the following implicit result,

$$q(t) = v_0 C \left[1 - \exp\left(-\frac{t}{\mathcal{R}_F C} + \frac{\eta \Delta \mathcal{R} q(t)}{\mathcal{R}_F Q_0}\right)\right], \tag{10}$$

where $\mathcal{R}_F = \mathcal{R}_0 - \eta \Delta \mathcal{R}(v_0 C)/Q_0$ is the memristance when $t \to \infty$. As before, equation (10) shows that when $eta = +1 (\eta = -1)$, the ideal MC circuit charges faster (slower) than an ideal RC circuit with the same resistance $\mathcal{R}_0$. In particular, the capacitor charging time for $\eta = +1$ (the doped region widens and the memristance reduces with time) decreases steeply as the dc voltage $v_0 \to Q_0(1 - w_0/D)/C$, the maximum voltage at which the linear-drift model is applicable.

Now we turn our attention to an ML circuit. Ideal RC and RL circuits are described by the same differential equation ($\mathrm{d}q/\mathrm{d}t + q/\tau_{RC} = 0$; $\mathrm{d}i/\mathrm{d}t + i/\tau_{RL} = 0$) with the same boundary conditions. Therefore, they have identical solutions [2] $q(t) = q_0 \exp(-t/\tau_{RC})$ and $i(t) = i_0 \exp(-t/\tau_{RL})$. As we will see below, this equivalence breaks down for MC and ML circuits. Let us consider an ideal ML circuit with initial current i_0. Kirchoff's voltage law implies that

$$Li \frac{\mathrm{d}i}{\mathrm{d}q} + \left(\mathcal{R}_0 - \eta \frac{\Delta \mathcal{R} q(t)}{Q_0}\right) i(t) = 0. \tag{11}$$

The solution of this equation above is given by $= Aq^2 - Bq + i_0 = (q - q_+)(q - q_-)$ where $A = \eta \Delta \mathcal{R}/2Q_0 L$, $B = \mathcal{R}_0/L$ and $q_\pm = (Q_0 \mathcal{R}_0/\Delta \mathcal{R})\left[1 \pm \sqrt{1 - 2\eta \Delta \mathcal{R} L i_0/Q_0 \mathcal{R}_0^2}\right]$ are the two real roots of $i(q) = 0$. We integrate the implicit result using partial fractions and get

$$q(t) = \frac{2Q_0 L i_0}{\Delta \mathcal{R}} \left[\frac{\mathrm{e}^{t/\tau_{ML}} - 1}{q_+ \mathrm{e}^{t/\tau_{ML}} - q_-}\right], \tag{12}$$

where $\tau_{ML} = L/\mathcal{R}_0 \sqrt{1 - 2\eta \Delta \mathcal{R} L i_0/Q_0 \mathcal{R}_0^2}$ is characteristic time associated with the ML circuit. The current $i(t)$ in the circuit is

$$i(t) = i_0 \left(\frac{2Q_0 L}{\Delta \mathcal{R} \tau_{ML}}\right)^2 \frac{\mathrm{e}^{t/\tau_{ML}}}{(q_+ \mathrm{e}^{t/\tau_{ML}} - q_-)^2}. \tag{13}$$

Equations (12) and (13) provide the set of analytical results for an ideal ML circuit. At small-t equation (13) becomes $i(t) = i_0(1 - t\mathcal{R}_0/L)$, whereas the large-$t$ expansion shows that the current decays exponentially, $i(t \to \infty) = i_0(2Q_0 L/q_+ \Delta \mathcal{R} \tau_{ML})^2 \exp(-t/\tau_{ML})$. Since τ_{ML} depends on the polarity of the memristor, $\tau_{ML}(\eta = +1) > \tau_{ML}(\eta = -1)$, the ML circuit with $\eta = +1$ discharges slower than its RL counterpart whereas the same ML circuit with $\eta = -1$ discharges faster than the RL counterpart. Figure 5 shows the theoretical i–t curves for an ML circuit obtained from equation (13); these results are consistent with our qualitative analysis. Note that the net charge passing through the memristor in an ML circuit is $q(t \to \infty) = q_-(i_0)$. Therefore, an upper limit on initial current i_0 for the validity of the linear-drift model is given by $q_-(i_0) \leqslant Q_0 w_0/D$ $(\eta = -1)$. As in the case of an ideal MC circuit charge, the ML circuit current decays steeply as i_0 approaches this upper limit.

Figures 4 and 5 suggest that ideal MC and ML circuits have a one-to-one correspondence analogous to the ideal RC and RL circuits. Therefore, it is tempting to think that the solution of an ideal ML circuit with a dc voltage v_0 is straightforward. (In a corresponding RL circuit,

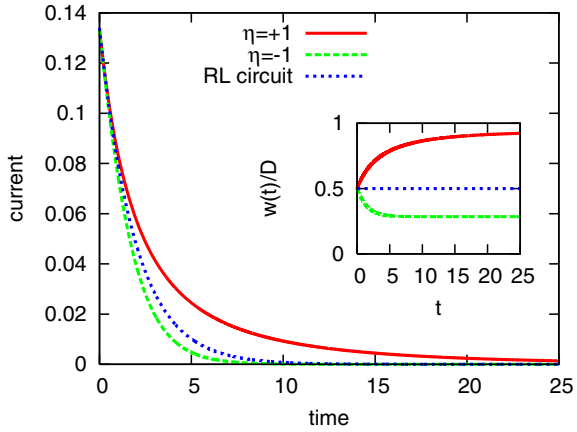

Figure 5. Theoretical i–t characteristics of an ideal ML circuit. The memristor parameters are $w_0/D = 0.5$ and $\mathcal{R}_{\rm OFF}/\mathcal{R}_{\rm ON} = 30$. The initial current in the circuit is small, $i_0/I_0 = 0.135$, to ensure the validity of the linear-drift model that breaks down when $i_0/I_0 > 0.140$ and $L/L_0 = 30$. The unit of inductance is $L_0 = \phi_0/I_0 = t_0\mathcal{R}_{\rm ON}$. We see that when $\eta = +1$ (red solid), the current in the ML circuit decays *slower* than when $\eta = -1$ (green dashed). The central blue dotted plot shows the exponential current decay of an RL circuit with the same initial resistance $\mathcal{R}_0$. The inset shows the time evolution of the boundary between the doped and undoped regions when $\eta = +1$ (red solid) and $\eta = -1$ (green dashed), and confirms that the linear-drift model is valid.

the current asymptotically approaches v_0/R for $t \gg \tau_{RL} = L/R$). The relevant differential equation obtained using Kirchoff's voltage law,

$$L\frac{{\rm d}i}{{\rm d}t} + \left(\mathcal{R}_0 - \eta\frac{\Delta\mathcal{R}q(t)}{Q_0}\right)i(t) = v_0, \tag{14}$$

shows that it is not the case. In an ML circuit, as the current $i(t)$ asymptotically approaches its maximum value, it can pump an arbitrarily large charge $q(t) = \int_0^t i(\tau)\,{\rm d}\tau$ through the memristor. Hence, for any nonzero voltage, no matter how small, the linear-drift model breaks down at large times when $w(t) = w_0 + \eta Dq(t)/Q_0$ exceeds D ($\eta = +1$) or becomes negative ($\eta = -1$). This failure of the linear-drift model reflects the fact that when the (oxygen vacancy) dopants approach either end of the memristor, their drift is strongly suppressed by a non-uniform electric field. Thus, unlike the ideal RL circuit, the steady-state current in an ideal ML circuit is not solely determined by the resistance $\mathcal{R}_0$ but also by the inductor. In the following section, we present more realistic models of the dopant drift that take into account its suppression near the memristor boundaries.

4. Models of nonlinear dopant drift

The linear-drift model used in preceding sections captures the majority of salient features of a memristor. It makes the ideal memristor, MC, and ML circuits analytically tractable and leads to closed-form results such as equations (7), (9) and (13). We leave it as an exercise for the reader to verify that these results reduce to their well-known R, RC and RL counterparts in the limit when the memristive effects are negligible, $\Delta\mathcal{R} \to 0$. The linear-drift model suffers from one serious drawback: it does not take into account the boundary effects. Qualitatively, the boundary between the doped and undoped regions moves with speed v_D in the bulk of the

memristor, but this speed is strongly suppressed when it approaches either edge, $w \sim 0$ or $w \sim D$. We modify equation (2) to reflect this suppression as follows [9]:

$$\frac{\mathrm{d}w}{\mathrm{d}t} = \eta \frac{\mu_D \mathcal{R}_{\mathrm{ON}}}{D} i(t) F\left(\frac{w}{D}\right). \tag{15}$$

The window function $F(x)$ satisfies $F(0) = F(1) = 0$ to ensure no drift at the boundaries. The function $F(x)$ is symmetric about $x = 1/2$ and monotonically increasing over the interval $0 \leqslant x \leqslant 1/2, 0 \leqslant F(x) \leqslant 1 = F(x = 1/2)$. These properties guarantee that the difference between this model and the linear-drift model, equation (2), vanishes in the bulk of the memristor as $w \to D/2$. Motivated by this physical picture, we consider a family of window functions parameterized by a positive integer p, $F_p(x) = 1 - (2x - 1)^{2p}$. Note that $F_p(x)$ satisfies all the constraints for any p. The equation $F_p(x) = 0$ has 2 real roots at $x = \pm 1$ and $2(p - 1)$ complex roots that occur in conjugate pairs. As p increases $F_p(x)$ is approximately constant over an increasing interval around $x = 1/2$ and as $p \to \infty$, $F_p(x) = 1$ for all x except at $x = 0, 1$. (For example, $1 - F_{p=16}(x) \geqslant 0.1$ only for $x \leqslant 0.035$ and $1 - x \leqslant 0.035$.) Thus, $F_p(x)$ with large p provides an excellent nonlinear generalization of the linear-drift model without suffering from its limitations. We note that at finite p, equation (15) describes a memristive system [4, 9] that is equivalent to an ideal memristor [3, 9] when $p \to \infty$ or when the linear-drift approximation is applicable. It is instructive to compare the results for large p with those for $p = 1$, $F_{p=1}(x) = 4x(1 - x)$, when the window function imposes a nonlinear drift over the *entire region* $0 \leqslant w \leqslant D$ [9]. For $p = 1$, it is possible to integrate equation (15) analytically and we obtain

$$w_{p=1}(q) = w_0 \frac{D \exp(4\eta q(t)/Q_0)}{D + w_0[\exp(4\eta q(t)/Q_0) - 1]}. \tag{16}$$

As expected, when the suppression at the boundaries is taken into account, the size of the doped region satisfies $0 \leqslant w(t) \leqslant D$ for all t and $w(t)$ asymptotically approaches $D(0)$ when $\eta = +1(-1)$. For $p > 1$, we numerically solve equation (15) with Kirchoff's voltage law applied to an ideal ML circuit

$$L\frac{\mathrm{d}i}{\mathrm{d}t} + M(q(t))i(t) = v(t), \tag{17}$$

using the following simple algorithm:

$$w_{j+1} = w_j + \eta \frac{\mu_D \mathcal{R}_{\mathrm{ON}}}{D} F\left(\frac{w_j}{D}\right) i_j, \epsilon_t \tag{18}$$

$$i_{j+1} = i_j + \frac{\epsilon_t}{L}[v_j - M(w_{j+1})i_j], \tag{19}$$

$$q_{j+1} = q_j + i_{j+1}\epsilon_t. \tag{20}$$

Here, ϵ_t is the discrete time step and w_j, i_j and q_j stand for the doped-region width, current and charge at time $t_j = j\epsilon_t$, respectively. The algorithm is stable and accurate for small $\epsilon_t \leqslant 10^{-2} t_0$.

Figure 6 compares the theoretical i–v results for a single memristor with two models for the dopant drift: a $p = 1$ model with non-uniform drift over the entire memristor (red solid) and a $p = 10$ model in which the dopant drift is heavily suppressed only near the boundaries (green dashed). We see that as p increases, beyond a critical voltage the memristance drops rapidly to $\mathcal{R}_{\mathrm{ON}}$ as the entire memristor is doped. Figure 7 shows theoretical results for a discharging ideal MC circuit obtained using two models: one with $p = 1$ (green dashed for $\eta = +1$ and blue dash-dotted for $\eta = -1$) and the other with $p = 10$ (red solid for $\eta = +1$ and magenta dotted for $\eta = -1$). The corresponding window functions $F_p(x)$ are shown in

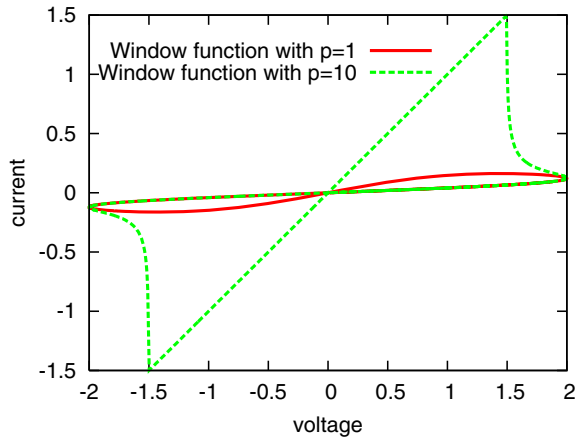

Figure 6. Theoretical i–v curves for a memristor with (realistic) dopant drift modelled by window functions $F_p(x) = 1 - (2x - 1)^{2p}$ with $p = 1$ (red solid) and $p = 10$ (green dashed), in the presence of an external voltage $v(t) = 2v_0 \sin(\omega_0 t/2)$. The memristor parameters are $w_0/D = 0.5$ and $\mathcal{R}_{\rm OFF}/\mathcal{R}_{\rm ON} = 50$. We see that the memristive behaviour is enhanced at $p = 10$. The slope of the i–v curves at small times is the same, $\mathcal{R}_0^{-1}$, in both cases whereas the slope on return sweep depends on the window function. For large p, the return-sweep slope is $\mathcal{R}_{\rm ON}^{-1} = 1 \gg \mathcal{R}_0^{-1}$ and it corresponds to a fully doped memristor.

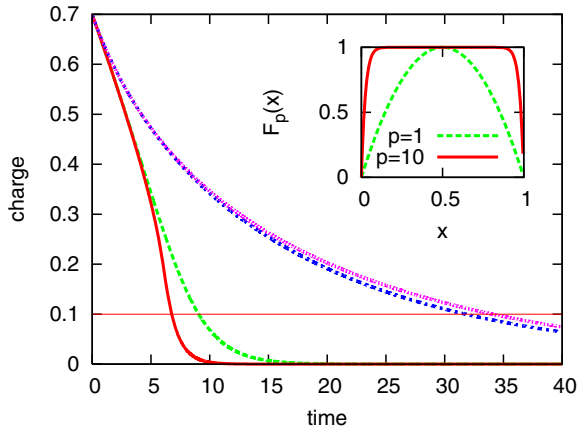

Figure 7. Theoretical q–t curves for an ideal MC circuit with nonlinear dopant drift modelled by window functions $F_p(x)$ with $p = 1$ and $p = 10$ shown in the inset. The green dashed ($\eta = +1$) and the blue dash-dotted ($\eta = -1$) correspond to the $p = 1$ window function. The red solid ($\eta = +1$) and the magenta dotted ($\eta = -1$) correspond to the $p = 10$ window function. The horizontal line at $q/Q_0 = 0.1$ is a guide to the eye. The memristor parameters are $w_0/D = 0.5$ and $\mathcal{R}_{\rm OFF}/\mathcal{R}_{\rm ON} = 20$. The initial charge on the capacitor is $q_0/Q_0 = 0.7$ and $C/C_0 = 1$. We see that the memristive effect is enhanced for large p when $\eta = +1$. Hence, for large p the two decay time scales associated with $\eta = +1$ (red solid) and $\eta = -1$ (magenta dotted) can differ by a factor of $\mathcal{R}_0/\mathcal{R}_{\rm ON} \gg 1$. Fitting the experimental data to these results can determine the nature of dopant drift in actual samples.

the inset. We observe that the memristive behaviour is enhanced as p increases, leading to a dramatic difference between the decay times of a single MC circuit when $\eta = +1$ (red solid) and $\eta = -1$ (magenta dotted). Figure 7 also shows that fitting the experimental data to these

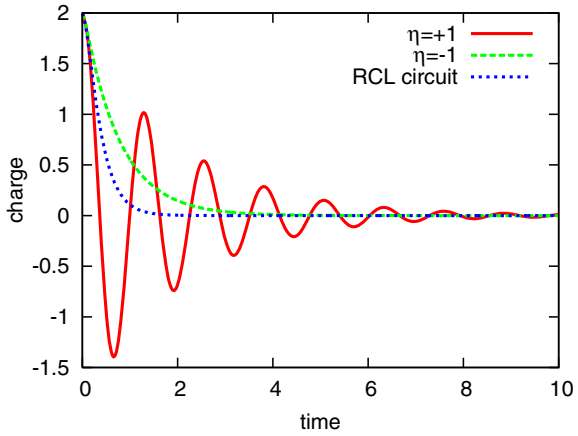

Figure 8. Theoretical q–t curves for an ideal discharging MCL circuit modelled using the window function for $p = 50$. The circuit parameters are $w_0/D = 0.5, \mathcal{R}_{\rm OFF}/\mathcal{R}_{\rm ON} = 20, L/L_0 = 1$, $C/C_0 = 0.04$ and $q_0/Q_0 = 2$. The initial resistance $\mathcal{R}_0 = 10.5$ implies that the corresponding ideal RCL circuit, with $\omega_{LC} = 1/\sqrt{LC} \sim \mathcal{R}_0/2L$, is close to critically damped. When $\eta = +1$ (red solid), we see that the MCL circuit is underdamped, whereas when $\eta = -1$ (green dashed) it is overdamped. Result for the RCL circuit with the same initial resistance $\mathcal{R}_0$ is shown by the blue dotted line. Thus, a single MCL circuit can be driven from overdamped to underdamped behaviour by simply exchanging the $\pm$ plates on the capacitor.

theoretical results can determine the window function that best captures the realistic dopant drift for a given sample.

The properties of ideal MC and ML circuits with an arbitrary voltage are obtained by integrating equations (15) and (17) using the algorithm described above. However, as the discussion in section 1 shows, these circuits significantly differ from their ideal RC and RL counterparts only at low frequencies.

5. Oscillations and damping in an MCL circuit

In this section, we discuss the last remaining elementary circuit, namely an ideal MCL circuit. First, let us recall the results for an ideal RCL circuit [1]. For a circuit with no voltage source and an initial charge q_0, the time-dependent charge on the capacitor is given by

$$q(t) = \begin{cases} q_0\, \mathrm{e}^{-t/2\tau_{RL}} \cos(\tilde{\omega} t) & \tilde{\omega}^2 > 0 \\ q_0\, \mathrm{e}^{-t/2\tau_{RL}} \cosh(|\tilde{\omega}| t) & \tilde{\omega}^2 < 0, \end{cases} \tag{21}$$

where $\tilde{\omega}^2 = \omega_{LC}^2 - (2\tau_{RL})^{-2} > 0$ defines an underdamped circuit and $\tilde{\omega}^2 < 0$ defines an overdamped circuit. The two results are continuous at $\tilde{\omega} = 0$ (critically damped circuit). Thus, an RCL circuit is tuned through the critical damping when the resistance in the circuit is increased beyond $R_c = 2\sqrt{L/C}$.

The nonlinear differential equation describing an MCL circuit is obtained by adding the capacitor term to equation (17),

$$L\frac{\mathrm{d}i}{\mathrm{d}t} + M(q(t))i(t) + \frac{q(t)}{C} = v(t). \tag{22}$$

Due to the q-dependent memristance, equation (22) is not analytically solvable; we use the numerical algorithm mentioned earlier to obtain the solution. Figure 8 shows theoretical q–t curves for a *single MCL circuit* obtained by numerically integrating equations (15) and (17)

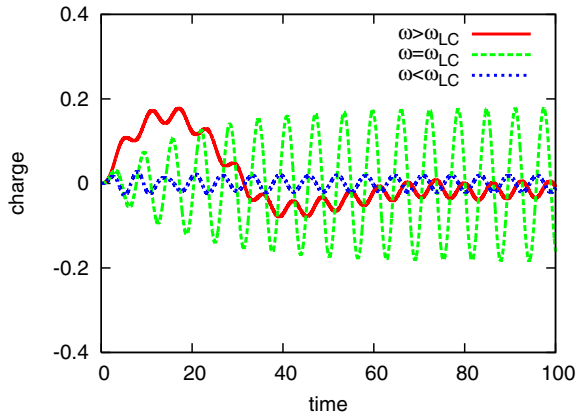

Figure 9. Theoretical q–t curves for an ideal MCL circuit driven by an ac voltage $v(t) = v_0 \sin(\omega_0 t)$ with $\eta = +1$. The circuit parameters $w_0/D = 0.5$, $\mathcal{R}_{\rm OFF}/\mathcal{R}_{\rm ON} = 10$, $L/L_0 = 50$ are fixed. The capacitance is $C/C_0 = 2$ (red solid), $C/C_0 = 0.02$ (green dashed) and $C/C_0 = 0.01$ (blue dotted). We see that for $\omega_{LC} < \omega_0$, the amplitude of the transient effects is comparable to the maximum amplitude that occurs at resonance, and that the memristive effect disappears in the steady-state solution.

using the $p = 50$ window function. When $\eta = +1$ (red solid), the circuit is underdamped because as the capacitor discharges the memristance reduces from its initial value $\mathcal{R}_0$. When $\eta = -1$ (dashed green), the discharging capacitor *increases* the memristance. Therefore, when $\eta = -1$ the MCL circuit is overdamped. For comparison, the blue dotted line shows the theoretical q–t result for an ideal RCL circuit with resistance $\mathcal{R}_0$ that is chosen such that the circuit is close to critically damped, $\mathcal{R}_0 \sim 2\sqrt{L/C}$. Figure 8 implies that if we exchange the $\pm$ plates of the capacitor in an MCL circuit, the charge will decay rapidly or oscillate. This property is unique to an MCL circuit and arises essentially due to the memristive effects.

For the sake of completeness, we briefly discuss the behaviour of an MCL circuit driven by an ac voltage source $v(t) = v_0 \sin(\omega t)$, with zero initial charge on the capacitor. For an ideal RCL circuit, the steady-state charge $q(t)$ oscillates with the driving frequency ω and amplitude $v_0/L\sqrt{\left(\omega^2 - \omega_{LC}^2\right)^2 + (\omega/\tau_{RL})^2}$. For a given circuit, the maximum amplitude $v_0\sqrt{LC}/R$ occurs at resonance, $\omega = \omega_{LC}$, and diverges as $R \to 0$ [1]. Figure 9 shows theoretical q–t curves for an ideal MCL circuit with $\eta = +1$ driven with $v(t) = v_0 \sin(\omega_0 t)$. The red solid line corresponds to low LC frequency $\omega_{LC} = 0.1\omega_0$, the dashed green line corresponds to resonance, $\omega_0 = \omega_{LC}$, and the dotted blue line corresponds to high LC frequency $\omega_{LC} = \sqrt{2}\omega_0$. We find that irrespective of the memristor polarity, the memristive effects are manifest only in the transient region. We leave it as an exercise for the reader to explore the strong transient response for $\omega_{LC} < \omega$ and compare it with the steady-state response at resonance $\omega_{LC} = \omega$.

6. Discussion

In this tutorial, we have presented the theoretical properties of the fourth ideal circuit element, the memristor, and of basic circuits that include a memristor. In keeping with the revered tradition in physics, the existence of an ideal memristor was predicted in 1971 [3] based purely

on symmetry arguments[4]; however, its experimental discovery [6–9] and the accompanying elegant physical picture [9, 11] took another 37 years. The circuits we discussed complement the standard RC, RL, LC, RCL circuits, thus covering all possible circuits that can be formed using the four ideal elements (a memristor, a resistor, a capacitor and an inductor) and a voltage source. We have shown in this tutorial that many phenomena—the change in the discharge rate of a capacitor when the $\pm$ plates are switched or the change in the current in a circuit when the battery terminals are swapped—are attributable to a memristive component in the circuit. In such cases, a real-world circuit can only be mapped onto one of the ideal circuits with memristors.

The primary property of the memristor is the *memory of the charge that has passed through it*, reflected in its effective resistance $M(q)$. Although the microscopic mechanisms for this memory can be different [9, 11], dimensional analysis implies that the memristor size D and mobility μ_D provide a unit of magnetic flux D^2/μ_D that characterizes the memristor. Although the underlying idea behind a memristor is straightforward, its nanoscale size remains the main challenge in creating and experimentally investigating basic electrical circuits discussed in this paper.

We conclude this tutorial by mentioning an alternate possibility. It is well known that an RCL circuit is equivalent [1] to a one-dimensional mass + spring system in which the position $y(t)$ of the point mass is equivalent to the charge $q(t)$, the mass is L, the spring constant is $1/C$ and the viscous drag force is given by $F(v) = -\gamma v$ where $\gamma = R$. Therefore, a memristor is equivalent to a viscous force with a y-dependent drag coefficient, $F_M = -\gamma(y)v$. Choosing $\gamma(y) = \gamma_0 - \Delta\gamma y/A$, where A is the typical stretch of the spring, will create the equivalent of an MCL circuit. Since a viscous force naturally occurs in fluids, a vertical mass + spring system in which the mass moves inside a fluid with a large vertical viscosity gradient can provide a macroscopic realization of the MCL circuit.

Acknowledgments

It is a pleasure to thank R Decca, A Gavrin, G Novak and K Vasavada for helpful comments. This work was supported by the IUPUI Undergraduate Research Opportunity Program (UROP). SJW acknowledges a UROP Summer Fellowship. YJ acknowledges Aspen Center for Physics, where part of the work was carried out, for their hospitality.

References

[1] See, for example, Walker J 2008 *Fundamentals of Physics* (New York: Wiley)
Young H D and Freedman R A 2008 *University Physics* (New York: Addison-Wesley)
Tipler P A and Mosca G 2008 *Physics for Scientists and Engineers* (New York: Freeman)
Ohanian H C and Markert J T 2008 *Physics for Engineers and Scientists* (New York: WW Norton)
[2] Feynman R P, Leighton R B and Sands M 1963 *The Feynman Lectures on Physics* vol II (New York: Addison-Wesley)
[3] Chua L O 1971 Memristor—the missing circuit element *IEEE Trans. Circuit Theory* **18** 507–19
[4] Chua L O and Kang S M 1976 Memristive devices and systems *Proc. IEEE* **64** 209–23
[5] Chua L O 1980 Device modeling via nonlinear circuit elements *IEEE Trans. Circuits Syst.* **27** 1014–44
[6] Thakoor S, Moopenn A, Daud T and Thakoor A P 1990 Solid-state thin film memristor for electronic neural networks *J. Appl. Phys.* **67** 3132–35
[7] Erokhin V V, Berzina T S and Fontana M P 2005 Hybrid electronic device based on polyaniline-polyethyleneoxide junction *J. Appl. Phys.* **97** 064501

[4] The displacement current in Maxwell's equations, a positron and a magnetic monopole are a few other historical examples whose existence was predicted purely based on symmetry principles. The first two have been experimentally observed, while the third one remains elusive.

[8] Erokhin V V, Berzina T S and Fontana M P 2007 Polymeric elements for adaptive networks *Cryst. Rep.* **52** 159–66
[9] Strukov D B, Snider G S, Stewart D R and Williams R S 2008 The missing memristor found *Nature* **453** 80–3
Tour J M and He T 2008 The fourth element *Nature* **453** 42–3
[10] Stewart D R, Ohlberg D A A, Beck P A, Chen Y, Williams R S, Jeppesen J O, Nielsen K A and Stoddart J F 2004 Molecule-independent electrical switching in Pt/organic monolayer/Ti devices' *Nano Lett.* **4** 133–6
[11] Pershin Y V and Di Ventra M 2008 Spin memristive systems *Phys. Rev.* B **78** 113309